JOURNAL OF SOLID STATE CHEMISTRY 81, 112–120 (1989)

Phase Transition Orthorhombic ↔ Rutile in Solid Solutions between $TaFeO_4$ or $TaVO_4$ and MnF_2

G. POURROY, P. POIX, AND S. MARIN

IPCMS Groupe de Chimie des Matériaux Inorganiques, UM380046 EHICS, 1 rue Blaise Pascal BP296, 67008 Strasbourg Cedex, France

Received December 15, 1988

Solid solutions $x TaMO_4$–$(1 - x)MnF_2$ with M = Fe and V exist in a limited domain ($x > 0.85$). The phases $x = 0.9$ have been synthesized and investigated by X-ray diffraction, transmission electron microscopy, and magnetic measurements. A phase transition orthorhombic ↔ rutile is reported in the iron compound at 750°C, while the vanadium phase is always rutile. The susceptibility of the latter follows a Curie–Weiss law above 150 K and presents a maximum at about 5 K. In the rutile iron compound, the paramagnetic domain is still not reached at 300 K. The orthorhombic phase is basically α-PbO_2 (*Pbcn*) and presents ferrimagnetism at low temperatures.

Introduction

Oxyfluoride compounds of general formula $TaMM'O_4F_2$ with M = Fe, V and M' = Ni have been recently studied and found to crystallize in the rutile structure at 650 and 700°C, respectively (*1*). Considering the difference between the oxidation degrees of tantalum on one hand and iron (or vanadium) and nickel on the other hand, we could expect a rearrangement along the c axis, thus giving a trirutile structure. This sort of order has been reported in MTa_2O_6 compounds (M = Fe, V, Ni) (*2–4*). Despite our efforts, we could not obtain any transformation in the vanadium case. As for the iron compound, its rutile structure transformed partly into an orthorhombic structure of α-PbO_2 type (space group *Pbcn*) at 550°C.

A simple mechanism for this transformation rutile → α-PbO_2 has been proposed by Galy and Anderson (*5*): 50% of the cations are shifted in the way indicated by the curved arrows in Fig. 1. The difference in their structure is that in rutile these strings of octahedra are straight in the c axis because they share opposite sides with each other, but in α-PbO_2, they are staggered along the a axis. It is now well known that cations like Mn^{2+}, Nb^{5+}, or Zn^{2+} prefer α-PbO_2 structure in AB_2O_6 compounds. Some of the latter crystallize both in rutile and α-PbO_2 structures, for instance, $NiNb_2O_6$, the rutile structure being the high-temperature form as in $TaFeNiO_4F_2$. Thus in order to study phase transition rutile → orthorhombic (α-PbO_2 type) and to obtain a complete transformation, we substitute Ni(II) for Mn(II). Structural and physical properties of solid solutions $x TaMO_4$–$(1 - x)MnF_2$ with M = Fe and V are reported in this paper.

Experimental

Solid solutions between $TaMO_4$ (M = Fe, V) and MnF_2 are prepared from the starting

0022-4596/89 $3.00

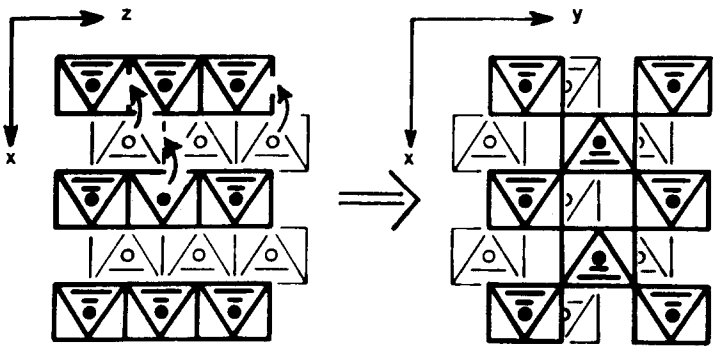

FIG. 1. Comparison of the rutile structure (left) with the α-PbO_2 structure type (right). Arrows indicate the possible cation movements for the transformation rutile → α-PbO_2. After Galy and Anderson (*5*).

compounds Ta_2O_5, M_2O_3 (M = Fe, V) and $MnF_2 \cdot MnF_2$ is synthesized using an original routine: manganese oxide, Mn_3O_4, or Mn_2O_3 and ammonium fluoride are ground together, put in a gold crucible, and introduced in an inconel tube (*6*). The mixture is heated at 150°C for 15 hr in an argon atmosphere. Oxide and fluoride strongly react, yielding a compact sample of ammonium double salts. By heating up to 720°C, the salts decompose, giving pure MnF_2. Tantalum oxide, Ta_2O_5, is obtained by dissolving tantalum chloride, $TaCl_5$, in anhydrous alcohol. The resulting solution is stirred while NH_4OH is added, giving thus a white precipitate of tantalum hydroxide. This powder is collected by filtration, then dried and heated. A very fine powder of well-crystallized Ta_2O_5 is obtained at 700°C. Iron oxide, Fe_2O_3, is synthesized by decomposition of iron(II) oxalate at 750°C. V_2O_3 is obtained by reduction of V_2O_5 under hydrogen atmosphere at 600°C for 1 day; the reduction is completely achieved at 1050°C.

Then MnF_2, Ta_2O_5, and M_2O_3 (M = Fe, V), taken in a stoichiometric ratio, are ground together, put in a gold crucible, and introduced in an inconel tube under an argon atmosphere. The samples are submitted to different thermal treatments listed in Table I. The second heating is always followed by a rapid cooling down to room temperature.

The samples are studied by means of X-

TABLE I

CHARACTERISTICS OF THE SOLID SOLUTIONS $x\text{Ta}M\text{O}_4$–$(1-x)\text{MnF}_2$(M = Fe, V): THERMAL TREATMENTS, STRUCTURES, AND COLORS

	$x\text{TaFeO}_4$–$(1-x)\text{MnF}_2$		$x\text{TaVO}_4$–$(1-x)\text{MnF}_2$	
Sample:	A $0 < x < 1$	B $x = 0.9$	C $0 < x < 1$	D $x = 0.9$
First heating	720°C 70 hr	720°C 70 hr	850°C 70 hr	850°C 70 hr
Second heating		950°C ½ hr		950°C ½ hr
Quenching		Yes		Yes
Structure	Orthorhombic	Rutile	Rutile	Rutile
Color	Yellow-brown		Black	

ray diffraction, transmission electron microscopy, and magnetic measurements. X-ray powder diffraction patterns have been taken using a Kristalloflex Siemens diffractometer and cobalt radiation. Magnetic susceptibility measurements were performed with a pendulum-type magnetometer in the temperature range 4.2–300 K and magnetization measurements were performed using a magnetometer designed in our laboratory.

General Characteristics of the Solid Solutions $x\mathrm{Ta}M\mathrm{O}_4$–$(1-x)\mathrm{MnF}_2$ (M = Fe, V)

The oxides Ta_2O_5 and Fe_2O_3 (or V_2O_3) taken alone react at about 1000–1100°C, depending on the granulometry of the powders, and give $TaFeO_4$ (or $TaVO_4$). When some MnF_2 is added, the reaction temperature strongly decreases. Some explanation was found after analyzing the iron compound formation. X-ray diffraction measurements showed that the fluoride MnF_2 first reacts with Ta_2O_5 probably giving some TaF_5, whose volatility makes the total synthesis easier.

No starting compounds are found in the sample $Ta_{0.9}M_{0.9}Mn_{0.1}O_{3.6}F_{0.2}$ heated at 750°C for M = Fe and 820°C for M = V. We obtain a single phase: an orthorhombic phase similar to the low-temperature phase of $TaFeNiO_4F_2$ for the iron compound (*1*) and a rutile phase for the vanadium compound. For $x < 0.85$, MnF_2 is detected in X-ray diffraction patterns. A simple calculation allows us to determine the limit of solid solutions in the iron case. After measuring the intensities of the most intensive reflections of each phases, we calculate the ratio $r = I(\mathrm{MnF_2})/I(\text{orthorhombic phase})$ for x = 0.1, 0.3, and 0.5. The zero value of r corresponds to the limit of the solid solution: we found $x = 0.83$. The result is quite similar in the vanadium case. So, in order to avoid little amounts of MnF_2 invisible in the X-ray diffraction pattern, which could distort magnetic measurements, we performed crystallographic and magnetic measurements on the sample $x = 0.9$.

Crystallographic and magnetic properties strongly depend on the thermal treatment particularly for the iron compounds. They present a phase transition orthorhombic → rutile above 750°C. But the transformation is very slow at this temperature. Furthermore, at the beginning of the transformation, the diffraction lines of the rutile structure are not symmetrical, particularly for the reflection 110. Therefore, a heating up to 950°C allows us to obtain rapidly a pure rutile phase. All our attempts to recover a pure orthorhombic phase by heating the rutile iron compound at lower temperature failed.

The vanadium solid solutions do not have the same behavior. Whatever the thermal treatment is, their structure is always rutile, but an accurate study of the lines shape in the diffraction pattern indicates that the structure is not a very pure rutile structure at 850°C (sample C), as it was observed for the iron compound. Furthermore, very weak diffraction lines corresponding to an orthorhombic structure appear in the diffraction pattern. So the structural study is carried out on sample D rapidly cooled down to room temperature.

Crystallographic Study of the Orthorhombic $Ta_{0.9}Fe_{0.9}Mn_{0.1}O_{3.6}F_{0.2}$ Phase

A powder diffraction pattern of the sample $Ta_{0.9}Fe_{0.9}Mn_{0.1}O_{3.6}F_{0.2}$ submitted to thermal treatment A was collected. The structure is orthorhombic, as is the structure of MnF_2 synthesized under pressure (*7*). The lattice parameters are given in Table II and the lattice spacings and their corresponding intensities in Table III. The lattice parameters are strongly reduced compared to those of MnF_2 (*7*), because of iron and tantalum cations which are smaller than manganese. The diffraction pattern is

TABLE II

CRYSTALLOGRAPHIC PARAMETERS AND VOLUME CELLS OF $Ta_{0.9}M_{0.9}Mn_{0.1}O_{3.6}F_{0.2}$ COMPARED WITH THOSE OF $TaMO_4$ AND MnF_2 (M = Fe, V)

Compound	Structure	a (Å)(±0.01)	b (Å)(±0.01)	c (Å)(±0.01)	V (Å^3)
$TaFeO_4$ (*12*)	Rutile	4.68_2		3.04_8	66.8
$TaVO_4$ (*13*)	Rutile	4.66_7		3.04_3	66.2
MnF_2 (*6*)	Rutile	4.86_7		3.30_8	78.3
MnF_2 (*7*)	α-PbO_2 (*Pbcn*)	4.96_0	5.80_0	5.35_9	77.0
$Ta_{0.9}Fe_{0.9}Mn_{0.1}O_{3.6}F_{0.2}$	Orthorhombic	4.65_0	5.62_0	5.02_9	65.7
	Rutile	4.68_8		3.05_8	67.2
$Ta_{0.9}V_{0.9}Mn_{0.1}O_{3.6}F_{0.2}$	Rutile	4.67_5		3.05_1	66.6

similar to the diffraction pattern of TaFe NiO_4F_2 at low temperatures, i.e., similar to the diffraction pattern of α-PbO_2 (space group *Pbcn*), but the reflections 010, 100, 011, and 120, forbidden in the latter structure, are not zero in our case. Nevertheless, we have computed the intensities of the reflection lines assuming a zero value for the forbidden reflections and a statistical distribution of the cations and the anions on sites 4c and 8d, respectively. The first three reflections have been eliminated because of the X-ray absorption at low angles. The smallest reliability factor $R = \Sigma|I_{calc} - I_{obs}|/\Sigma I_{obs} = 8.4\%$ has been obtained for the following positional parameters:

Cations: $x = 0.000$, $y = 0.171$, $z = 0.250$
Anions: $x = 0.250$, $y = 0.392$, $z = 0.402$.

These values are close to those encountered for MnF_2 (*8*) and PbO_2 (*9*), so that these results allow us to state positively that the structure is basically α-PbO_2. A schematic representation of the cell is given in Fig. 2.

The existence of reflections 100 and 011 has been confirmed by transmission electron microscopy (Fig. 3). The emergence of these diffraction lines may indicate that an order between the cations is appearing, but a longer annealing for 1 week at 650°C does not increase the intensities of the forbidden lines. So we cannot conclude about the origin of these reflections.

Crystallographic Study of the Rutile Phases $Ta_{0.9}M_{0.9}Mn_{0.1}O_{3.6}F_{0.2}$ (M = Fe,V)

The lattice parameters of the rutile phases are given in Table II. They are close to those of $TaMO_4$ (M = Fe, V), due to a small amount of MnF_2 involved in the compound. The lattice spacings and their corresponding intensities are listed in Table IV for the iron compound and Table V for the vanadium compound. The intensities have been computed assuming a statistical occupation of the metallic sites (2a) and a mean positional parameter x for the anions in site 4e. A distinction between the anionic sites

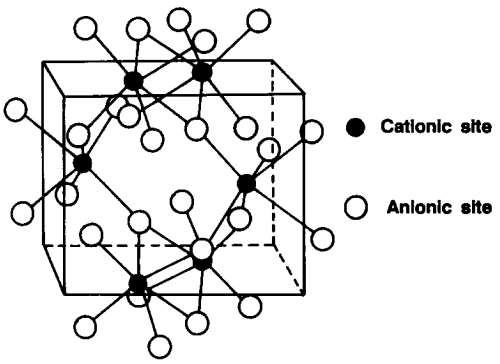

FIG. 2. Schematic representation of the orthorhombic α-PbO_2 cell.

TABLE III

EXPERIMENTAL AND CALCULATED LATTICE SPACINGS AND DIFFRACTION LINE INTENSITIES OF THE ORTHORHOMBIC PHASE $Ta_{0.9}Fe_{0.9}Mn_{0.1}O_{3.6}F_{0.2}$ (SPACE GROUP *Pbcn*)

hkl	d_{obs}	I_{obs}	d_{calc}	I_{calc}
010	5.60	1	5.62	0
100	4.65	3	4.65	0
011	3.745	2	3.748	0
110	3.58	28	3.583	28
111	2.916	100	2.918	100
020	2.809	8	2.810	7
002	2.512	15	2.515	18
021	2.451	19	2.453	19
120	2.387	<1	2.405	0
200	2.324	9	2.325	9
102	2.211	3	2.212	2
121	2.169	5	2.170	3
112	2.057	9	2.058	11
211	1.976	<1	1.976	<1
022	1.873	6	1.874	6
220	1.791	5	1.791	5
130	1.738	14	1.738	14
202	1.707	15	1.707	15
221	1.687	21	1.687	23
113	1.518	13	1.518	14
310	1.493	2	1.494	2
222	1.459	5	1.459	5
023	1.439	33	1.440	8
311	1.432		1.432	11
132	1.430		1.430	14
040	1.405	2	1.405	1
041	1.353	5	1.353	5
302	1.319	1	1.319	1
321	1.310	<1	1.310	<1
312	1.284	3	1.285	2
004	1.257	2	1.257	2
223	1.224	4	1.224	4
042	1.224		1.227	1
330	1.194	6	1.194	4
114	1.186		1.186	2
241	1.169	10	1.170	7
400	1.162		1.163	3
024	1.147	1	1.148	1
313	1.115	5	1.115	6
204	1.106	5	1.106	5
150	1.093	1	1.093	1
242	1.085	13	1.085	2
332	1.078		1.079	8
043	1.076		1.077	3
420	1.074		1.074	1
151	1.068	5	1.068	5
402	1.055	9	1.055	4
421	1.050		1.051	5

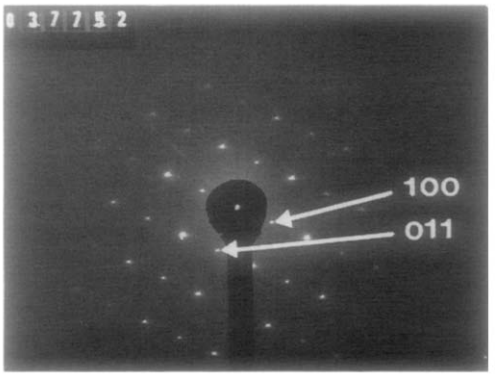

FIG. 3. Electron diffraction pattern of the orthorhombic phase $Ta_{0.9}Fe_{0.9}Mn_{0.1}O_{3.6}F_{0.2}$.

has not been taken into account since it does not modify the intensities to a great extent. The two first diffraction lines have been eliminated from the calculation because of the X-ray absorption at low angles.

TABLE IV

EXPERIMENTAL AND CALCULATED LATTICE SPACINGS AND DIFFRACTION LINE INTENSITIES OF THE RUTILE PHASE $Ta_{0.9}Fe_{0.9}Mn_{0.1}O_{3.6}F_{0.2}$ (SPACE GROUP $P4_2/mnm$)

hkl	d_{obs}	I_{obs}	d_{calc}	I_{calc}
110	3.307	127	3.315	148
011	2.557	100	2.561	125
200	2.341	28	2.344	33
111	2.245	8	2.248	6
120	2.094	2	2.097	1
121	1.728	100	1.729	100
220	1.657	26	1.658	27
002	1.528	10	1.529	11
130	1.481	22	1.483	26
301	1.390	56	1.3915	30
112	1.387		1.388	23
202	1.281	13	1.281	13
231	1.1965	25	1.1966	27
400	1.172	10	1.172	10
222	1.124	20	1.1238	20
330	1.105	9	1.105	9
141	1.065	61	1.0657	31
132			1.0643	31
240	1.0486	14	1.0483	14
103	0.9965	18	0.9961	18
402	0.9307	35	0.9300	35

TABLE V

EXPERIMENTAL AND CALCULATED LATTICE SPACINGS AND DIFFRACTION LINE INTENSITIES OF THE RUTILE PHASE $Ta_{0.9}V_{0.9}Mn_{0.1}O_{3.6}F_{0.2}$ (SPACE GROUP $P4_2/mnm$)

hkl	d_{obs}	I_{obs}	d_{calc}	I_{calc}
110	3.303	139	3.306	157
011	2.553	104	2.555	126
200	2.336	30	2.338	35
111	2.240	7	2.242	6
120	2.089	2	2.091	2
121	1.724	100	1.725	100
220	1.653	26	1.653	26
002	1.525	12	1.526	11
130	1.478	24	1.478	27
301	1.386	52	1.388	29
112			1.385	23
202	1.280	11	1.278	13
231	1.193	24	1.193	24
400	1.169	10	1.169	8
222	1.121	19	1.121	18
330	1.102	9	1.102	9
141	1.062	56	1.063	28
132			1.062	27
240	1.0456	14	1.0454	13
103	0.9940	14	0.9938	15
402	0.9277	29	0.9278	29

The smallest reliability factors R have been obtained with $x = 0.290$ ($R = 4.7\%$) and $x = 0.297$ ($R = 4.5\%$) for the iron and vanadium compounds, respectively.

Magnetic Properties

Magnetic measurements performed at room temperature showed that the samples $Ta_{0.9}M_{0.9}Mn_{0.1}O_{3.6}F_{0.2}$ (M = Fe, V) do not present any ferromagnetic components. Their magnetic behaviors versus temperature strongly depend on the crystallographic structure and the cation M involved in the compound. The raw data are corrected from the diamagnetism according to the Slater and Angus method: χ_{dia} is equal to 75×10^{-6} emu/mol for both compounds (*10*).

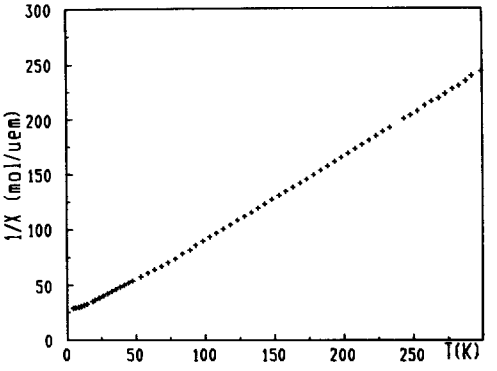

FIG. 4. Inverse susceptibility of $Ta_{0.9}V_{0.9}Mn_{0.1}O_{3.6}F_{0.2}$ versus temperature.

The most simple behavior is encountered for the vanadium rutile phase. The susceptibility follows a Curie–Weiss law above 150 K, $\chi = 1.28/(T + 15)$, and exhibits a maximum at about 5 K (Fig. 4).

The iron rutile phase has a similar behavior, but paramagnetism occurs at temperatures higher than 300 K (Fig. 5). No maximum in the susceptibility curve has been pointed out in the temperature range 4.2–300 K.

As for the orthorhombic $Ta_{0.9}Fe_{0.9}Mn_{0.1}O_{3.6}F_{0.2}$ phase, its behavior is completely different: the magnetic moment strongly increases under 160 K when the temperature decreases (Fig. 6). Under 20 K, the suscep-

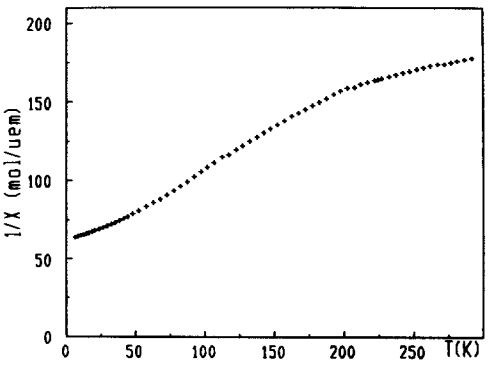

FIG. 5. Inverse susceptibility of $Ta_{0.9}Fe_{0.9}Mn_{0.1}O_{3.6}F_{0.2}$ versus temperature.

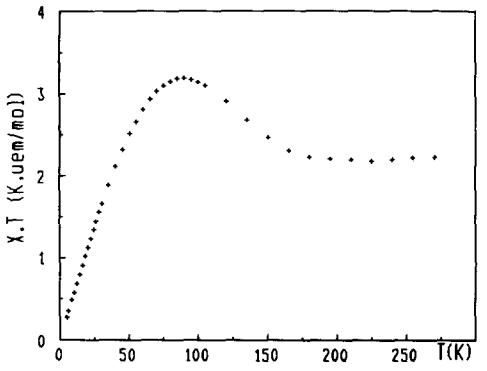

FIG. 6. Magnetic moment of $Ta_{0.9}Fe_{0.9}Mn_{0.1}O_{3.6}F_{0.2}$ versus temperature.

tibility takes a quasiconstant value and the magnetization strongly depends on the applied magnetic field. At 6 K, the sample $Ta_{0.9}Fe_{0.9}Mn_{0.1}O_{3.6}F_{0.2}$ is characterized by a coercive field of 1500G and a magnetic moment of 3.53 uem/g, i.e., 0.177 μ_B/mole at high magnetic field, as we can see it on the hysteresis curve (Fig. 7).

Discussions and Conclusions

The solid solutions $x\text{Ta}M\text{O}_4$–$(1 - x)$ MnF_2 (M = Fe, V) between the rutile phases $TaFeO_4$ or $TaVO_4$ on one hand and MnF_2 on the other hand exist in a limited domain ($x > 0.85$). This is not surprising since the characteristic cation–oxygen lengths are greater for manganese (2.22 Å) than for tantalum (2.016 Å) and iron (2.02 Å (*11*). They present either an orthorhombic or a rutile structure depending on the thermal treatment and the metallic cation involved. The orthorhombic phase is a low-temperature phase in $Ta_{0.9}Fe_{0.9}Mn_{0.1}O_{3.6}F_{0.2}$ as well as in $TaFeNiO_4F_2$ (*1*), but it is pure and more easily obtained with the former. Furthermore, when iron is replaced by vanadium and whatever the thermal treatment is, we cannot obtain an orthorhombic phase. So, these results allow us to classify the cations according to their structural preference: Mn^{2+} and Fe^{3+} favor the orthorhombic α-PbO_2 structural type, while Ni^{2+} and V^{3+} prefer the rutile structure. This is in total agreement with what is observed for the oxides AB_2O_6. Indeed, $MnTa_2O_6$ (*14*) and Fe_2WO_6 (*15*) crystallize in a columbite and a tri-α-PbO_2 structure, respectively (both have a α-PbO_2 basic cell), while $NiTa_2O_6$ (*4*) and V_2WO_6 (*16*) prefer a trirutile structure.

Therefore, the oxyfluoride phases we have obtained to date always present a rutile structure. For $Ta_{0.9}Fe_{0.9}Mn_{0.9}O_{3.6}F_{0.2}$, it is a high-temperature phase appearing

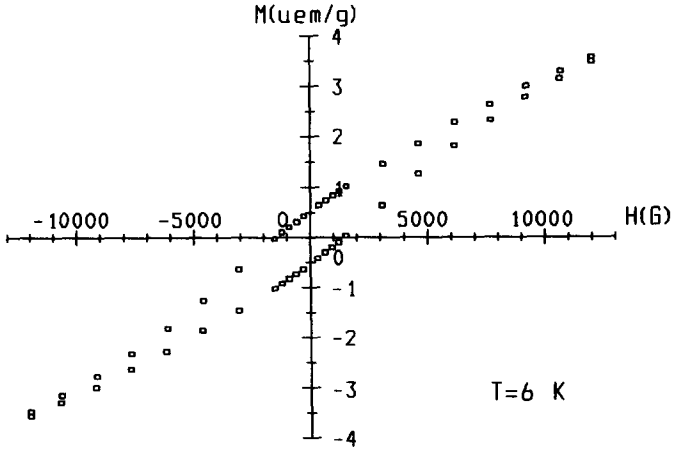

FIG. 7. Magnetic field dependence of the magnetization of $Ta_{0.9}Fe_{0.9}Mn_{0.1}O_{3.6}F_{0.2}$ at 6 K.

above 750°C. This phase transition orthorhombic → rutile has a very slow reaction rate at this temperature such as the inverse transformation. Indeed, we cannot recover a pure orthorhombic phase for the rutile compound by heating it at 650°C for a week.

The crystallographic study performed on the orthorhombic $Ta_{0.9}Fe_{0.9}Mn_{0.9}O_{3.6}F_{0.2}$ does not allow us to determine the space group. After the computation of the intensities of the diffraction lines, the structure is basically α-PbO_2, but the emergence of the forbidden lines 010, 100, 011, and 120, confirmed by transmission electron microscopy, shows that *Pbcn* is not the true space group. Indeed, the conditions limiting the reflections $0kl$ ($k = 2n$) and $hk0$ ($h + k = 2n$) are no more fulfilled. The space group *Pmma* could correspond to the new conditions. Thus, the cations would occupy sites 2f and 2e and the anions sites 8l, i.e., all sites 4c in the orthorhombic cell (Fig. 2) would no longer be equivalent. There would be a segregation between the cations, due to the different sizes and electronic charges between Mn^{2+} and Ta^{5+}. The existence of two different sublattices can explain the field dependent magnetization at low temperatures. The shape of the hysteresis curve obtained at 6 K indicates that the coercitive field is not negligible and the saturation still not reached. So the magnetic moment measured at high magnetic fields does not correspond to the difference between the magnetic moments of the sublattices. It is probably due to the closeness of the Curie point. As the susceptibility is quasiconstant under 20 K, it presumably takes place under 20 K. More accurate studies of crystallographic structure and magnetic properties must be carried out to conclude definitely about the nature of the sublattices.

In any case, the magnetic moments measured at room temperature, 2.25 for the orthorhombic iron compound and 1.7 for the rutile iron oxyfluoride, allow us to state that the interactions between iron and manganese cations are strong. All spins are not decoupled at room temperature in the iron compound, contrary to the spins in the vanadium oxyfluoride. Indeed, the latter follows a Curie–Weiss law above 150 K with a Curie constant close to the theoretical value $C_{th} = 1.3375$. This difference was already observed between vanadium and iron in $TaMNiO_4F_2$ (M = Fe, V) oxyfluorides (*1*): the Curie constant is reduced in the iron compound $C_{calc} = 4.70$ and $C_{th} = 5.375$ and not in the vanadium compound. This behavior can be explained considering the fact that both iron phases $TaFeNiO_4F_2$ and $Ta_{0.9}Fe_{0.9}Mn_{0.1}O_{3.6}F_{0.2}$ present the transition orthorhombic ↔ rutile. The cationic sequence of the orthorhombic phase is probably encountered on short distances in the rutile phase, so that metallic ions are not statistically distributed in sites 2a. A statistical distribution in the rutile $Ta_{0.9}Fe_{0.9}Mn_{0.1}O_{3.6}F_{0.2}$ phase would imply that most magnetic cations are isolated between diamagnetic tantalum ions because the ratio [diamagnetic ion]/[paramagnetic ion] is close to 1, so that the magnetic behavior would have to be close to the monomer $S = 5/2$ magnetic behavior. The variation of the inverse susceptibility allows us to state that the cationic distribution is probably not statistical in the rutile iron phase. A more statistical distribution presumably requires higher synthesis temperatures or longer annealings.

All these physical properties will be better understood by continuing investigations on other solid solutions, for instance, by replacing tantalum by niobium or manganese by iron or zinc. These studies are now in progress in our laboratory.

Acknowledgments

We thank G. Ehret C.S.G.S. Strasbourg for electron diffraction patterns, A. Derory IPCMS G.C.M.I.

UM380046 EHICS Strasbourg for recording magnetization measurements, and I. Fettig I.U.T. Chimie Strasbourg for her technical help.

References

1. G. POURROY, P. POIX, AND J. P. SANCHEZ, *J. Solid State Chem.* **74,** 27 (1988).
2. H. WEITZEL AND S. KLEIN, *Acta Crystallogr. Sect. A* **30,** 380 (1974).
3. J. C. BERNIER AND P. POIX, *C.R. Acad. Sci. Paris* **265,** 1164 (1967).
4. R. K. KREMER AND J. E. GREEDAN, *J. Solid State Chem.* **73,** 579 (1988).
5. J. GALY AND S. ANDERSON, *J. Solid State Chem.* **3,** 525 (1971).
6. G. POURROY AND P. POIX, *J. Fluorine Chem.* **42,** 257 (1989).
7. D. P. DANDEKAR AND J. C. JAMIESON, *in* "Proc., Symposium on Crystal Structure at High Pressure, Seattle, March 24, 1969—Trans. Amer. Cryst. Assoc. (1969).
8. Structure Reports 28, 72.
9. Structure Reports 17, 388.
10. J. C. BERNIER AND P. POIX, *Actual. Chim.* **2,** 7 (1978).
11. P. POIX, *C.R. Acad. Sci.* **268,** 1139 (1969).
12. M. GRILLET, Thèse 3e cycle Paris XI (1974).
13. H. TRARIEUX, J. C. BERNIER, AND A. MICHEL, *Ann. Chim.* **4,** 183 (1969).
14. H. WEITZEL AND S. KLEIN, *Solid State Commun.* **12,** 113 (1973).
15. J. GALY AND J. SENEGAS, *J. Solid State Chem.* **10,** 5 (1974).
16. J. C. BERNIER AND P. POIX, *C.R. Acad. Sci. Paris* **265,** 1247 (1967).